

# On-Top $\pi$ -Stacking of Quasiplanar Molecules in Hole-Transporting Materials: Inducing Anisotropic Carrier Mobility in Amorphous Films

Atsushi Wakamiya,\* Hidetaka Nishimura, Tatsuya Fukushima, Furitsu Suzuki, Akinori Saeki, Shu Seki, Itaru Osaka, Takahiro Sasamori, Michihisa Murata, Yasujiro Murata,\* and Hironori Kaji\*

((Dedication----optional))

**Abstract:** Dimers of partially oxygen-bridged triarylamines were designed and synthesized as hole-transporting materials. X-ray structural analyses revealed that these compounds form on-top  $\pi$ -stacking aggregates in the crystalline state. TRMC measurements exhibited that high levels of anisotropic charge-transport were induced in direction of the  $\pi$ -stacking. Surprisingly, even in vacuum deposited amorphous films, these compounds retained some of the face-on  $\pi$ -stacking, thus facilitating an out-of-plane carrier mobility.

The development and characterization of improved charge-transporting materials still remains a crucial issue for the achievement of high performance in organic-device applications, e.g. organic light-emitting diodes (OLEDs),<sup>[1]</sup> organic field-effect transistors (OFETs)<sup>[2]</sup> and organic photovoltaics (OPVs).<sup>[3]</sup> Efficient charge transport in molecular solids requires charges to move easily from molecule to molecule.<sup>[4]</sup> In the molecular design of these

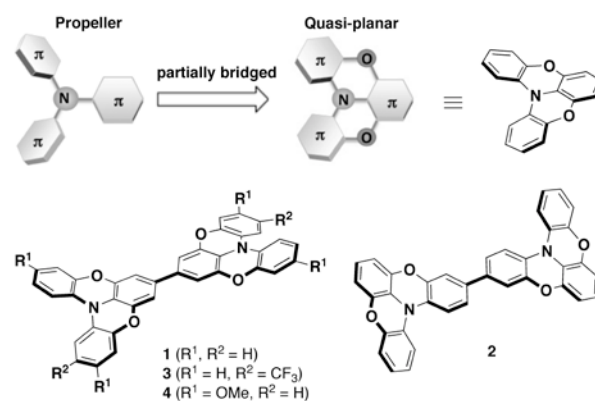


**Figure 1.** Molecular design aspects for charge-transporting materials with a quasi-planar structure as the key feature.

[\*] Prof. Dr. A., Wakamiya, H. Nishimura, Dr. T. Fukushima, F. Suzuki, Prof. Dr. T. Sasamori, Dr. M. Murata, Prof. Dr. Y. Murata, Prof. Dr. H. Kaji  
Institute for Chemical Research, Kyoto University  
Uji, Kyoto 611-0011 (Japan)  
E-mail: wakamiya@scl.kyoto-u.ac.jp, yasujiro@scl.kyoto-u.ac.jp, kaji@scl.kyoto-u.ac.jp

Dr. A. Saeki, Prof. Dr. S. Seki  
Department of Applied Chemistry, Graduate School of Engineering, Osaka University  
2-1 Yamadaoka, Suita, Osaka 565-0871 (Japan)

Dr. I. Osaka  
Emergent Molecular Function Research Group, RIKEN CEMS  
Wako, Saitama 351-0198 (Japan)

Prof. Dr. A. Wakamiya  
Precursory Research for Embryonic Science and Technology (PRESTO), Japan Science and Technology Agency  
4-1-8 Honcho, Kawaguchi, Saitama 332-0012 (Japan)

[\*\*] This work was partially supported by JST, and the Collaborative Research Program at the ICR, Kyoto Univ. Support was also received from the Funding Program for World Leading Innovative R&D on Science and Technology (FIRST Program). The NMR measurements were supported by the Joint Usage/Research Center (JURC) at the ICR, Kyoto Univ. Synchrotron single-crystal X-ray analysis was carried out with the SPring-8 beam line BL38B1 with the approval of JASRI (2012A1448, 2012B1319, and 2013A1489). 2D-GIXD experiments were performed at BL19B2 of SPring-8 with the approval of JASRI (2013A1634). We thank Dr. T. Koganezawa (JASRI) for advice on the 2D-GIXD measurements.



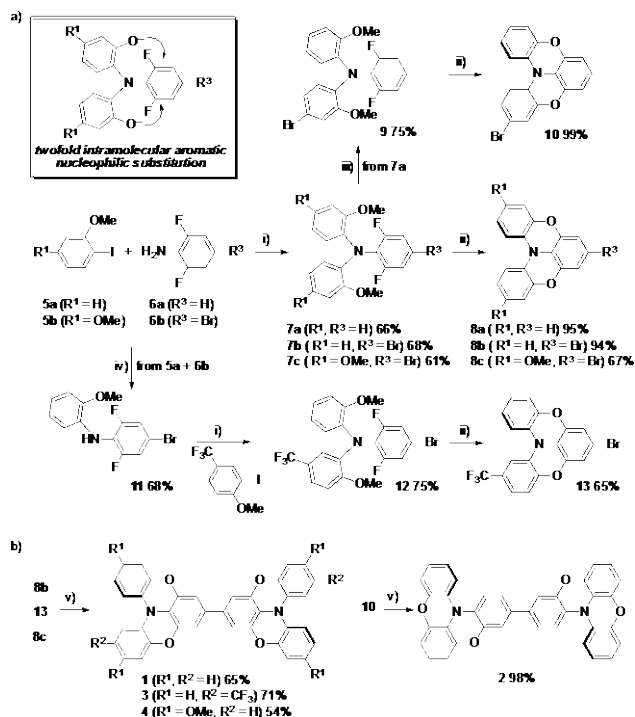
Supporting information for this article is available on the WWW under <http://www.angewandte.org>

materials, it is therefore important, not only to control the  $\pi$ -electronic structure for the tuning of the HOMO and LUMO levels and the lowering of the reorganization energy ( $\lambda$ ), but also to control the packing structure in the solid state, in order to facilitate large charge transfer integrals ( $J$ ). Acenes, such as pentacene for example, are widely used as charge-transporting materials in OFETs, due to their rigid  $\pi$ -conjugated skeletons with high planarity. In the solid state, pentacene adopts a herringbone structure with a tilted molecular arrangement, which is the result of  $\pi$ - $\pi$  interactions and the presence of CH- $\pi$  interactions (electrostatic interaction).<sup>[5]</sup> Introducing substituents in the peri position of acenes, or increasing the C/H ratio of ring-fused aromatic compounds can be effective strategies for a molecular design, in which CH- $\pi$  interactions are prevented and a better packing motif with facilitated charge mobility is obtained.<sup>[2,6]</sup> However, molecular design approaches allowing effective control over the molecular orientation in the solid state remain limited. Representative examples for hole-transporting materials used in OLEDs are triarylamines with propeller-like structures, such as TPD<sup>[7a]</sup> and  $\alpha$ -NPD.<sup>[7b]</sup> These materials are used as amorphous films, and the conformations of individual molecules as well as of their aggregates have not been determined unambiguously, rendering precise conclusions with respect to molecular design strategies difficult.<sup>[8]</sup> Accordingly, the elucidation of the exact relationship between molecular orientation in the crystalline and amorphous state remains a key challenge to be addressed in the design of advanced charge-transporting materials.

In this study, we focused on partially bridged triarylamines as the  $\pi$ -conjugated skeletons for the charge-transporting materials. In these amines, three phenyl groups are constrained in a quasi-planar fashion by two oxygen-bridges (Figure 1). We envisioned that the use of quasi-planar scaffolds should be beneficial in order to provide: a) delocalized  $\pi$ -conjugation by enhanced planarity, and b) dense  $\pi$ -stacking in the solid state, arising from slightly twisted molecular structures. In addition, the dispersion in the direction of

the C-H bonds in the lateral position of the quasi-planar molecules should decrease the contribution of CH- $\pi$  interactions between neighbouring molecules, so that on-top  $\pi$ -stacking could be facilitated in the solid state. As model compounds, we designed and synthesized a series of partially oxygen-bridged triarylamine dimers **1–4** (Figure 1). Herein, we report results on the characterization of **1–4** in solution and solid state, as well as on the relationship between the packing structures and the anisotropic charge carrier-transport properties, which were observed for **1** and **2** both in the crystalline and amorphous state.

The key reaction step in order to establish quasi-planar structures in **8a–c**, is a twofold intramolecular nucleophilic aromatic substitution (Scheme 1a). Compounds **7a–c** were prepared by Ullmann reactions of **5a–b** and **6a–b** (61–68%). After removal of the protecting methyl groups in **7a–c** with  $\text{BBr}_3$ , a subsequent treatment with  $\text{K}_2\text{CO}_3$  in DMF at 100 °C resulted in the formation of cyclized products **8a–c** (67–95%). This synthetic route is straightforward, based on commercially available starting materials and is easily scaled up. In contrast to a previously reported synthetic route for **8a** via the linear intermediate 2,6-bis(2-bromophenoxy)aniline,<sup>[9]</sup> our route allows the preparation of derivatives containing substituents in the desired positions. For example, the bromination of triarylamine **7a** with 1 equiv. of NBS resulted in the selective formation of **9** (75%). The subsequent twofold cyclization of **9** gave monobrominated **10**, an isomer of **8b**, in almost quantitative yield. The unsymmetric triarylamine **13** was obtained from two successive coupling reactions of **6b** with different aryl components. Pd(0)-catalyzed arylation of **5a** with **6b** resulted in the selective formation of **11** (68%). A subsequent second Ullmann arylation afforded **12** (75%), which was doubly cyclized to give **13** (65%). Homo-coupling of brominated **8b–c**, **10**, and **13** yielded the corresponding dimers **1–4** (54–98%) as pale



**Scheme 1.** Reagents/conditions: i) Cu,  $\text{K}_2\text{CO}_3$ , *o*-dichlorobenzene, 180 °C; ii) 1.  $\text{BBr}_3$ ,  $\text{CH}_2\text{Cl}_2$ , 2.  $\text{K}_2\text{CO}_3$ , DMF, 100 °C, (then  $\text{CH}_3\text{I}$ , 60 °C for **8c**); iii) NBS (1 equiv.),  $\text{CHCl}_3/\text{AcOH}$ , iv)  $\text{Pd}_2(\text{dba})_3 \cdot \text{CHCl}_3$ ,  $\text{P}(t\text{-Bu})_3$ ,  $\text{NaOt-Bu}$ , toluene, 100 °C; v)  $\text{Ni}(\text{cod})_2$ , bipyridine, COD, THF, 60 °C. NBS = *N*-bromosuccinimide, dba = *trans,trans*-dibenzylideneacetone, cod = cycloocta-1,5-diene.

**Table 1:** Thermal analysis, electrochemical and photophysical data for **1–4**.

	$T_{\text{d}5}^{\text{[a]}}$ [°C]	$T_{\text{g}}^{\text{[b]}}$ [°C]	$E_{1/2, \text{ox}}^{\text{[c]}}$ [V]	IP <sup>[d]</sup> [eV]	Abs <sup>[e]</sup> [nm] (log $\epsilon$ )	FL <sub>liq</sub> <sup>[e]</sup> [nm] ( $\phi$ ) <sup>[g]</sup>	FL <sub>sol</sub> <sup>[f]</sup> [nm] ( $\phi$ ) <sup>[g]</sup>
<b>1</b>	449	64	+0.25 +0.44	5.05	387 (4.22)	451 (0.51)	491 (0.40)
<b>2</b>	441	123	+0.23 +0.42	5.03	397 (4.48)	449 (0.69)	508 (0.51)
<b>3</b>	408	56	+0.41 +0.58	5.21	385 (4.16)	439 (0.45)	485 (0.14)
<b>4</b>	443	34	+0.02 +0.17 +0.86 <sup>[h]</sup>	4.82	405 (4.10)	489 (0.77)	533 (0.19)

[a] 5% weight loss temperature measured by TGA. [b] Glass transition temperature measured by DSC. [c] Half-wave oxidation potential (vs.  $\text{Fc}/\text{Fc}^+$ ) measured by CV in  $\text{CH}_2\text{Cl}_2$  (0.3 mM) with  $[(n\text{-Bu})_4\text{N}][\text{PF}_6]$  (0.1 M) as the supporting electrolyte. [d] Estimated IPs from the first oxidation potential (+4.80 eV).<sup>[10]</sup> [e] UV absorption/fluorescence measured in  $\text{CH}_2\text{Cl}_2$ . [f] Fluorescence measured in the solid state (grinded crystals). [g] Absolute quantum yields determined by a calibrated sphere system. [h] Corresponding to a two electron oxidation.

yellow solids (Scheme 1b).

The electrochemical and photophysical data as well as thermal analysis for **1–4** are summarized in Table 1. A detailed discussion of these properties can be found in the supporting information.

The optimized structures of **1–4**, calculated at the B3LYP/6-31G(d) level of theory, supported the expected quasi-planar structures for the partially oxygen-bridged triarylamine moieties (Figure S17). The HOMOs of **1–4** are highly delocalized over the whole  $\pi$ -skeleton (Figure S18), which allows an effective tuning of the HOMO levels via the peripheral substituents on the outer phenyl rings. Fully delocalized HOMOs should also lower the reorganization energies of the hole-transfer. For **1–4**, these were calculated at the B3LYP/6-31G(d) level to be lower (**1**:  $\lambda^+ = 0.15$  eV; **2**: 0.15 eV; **3**: 0.18 eV; **4**: 0.17 eV) than those for TPD ( $\lambda^+ = 0.26$  eV) or  $\alpha$ -NPD ( $\lambda^+ = 0.28$  eV).

Single crystals of **1–4**, suitable for X-ray diffraction analysis, were obtained by sublimation or recrystallization. The structural analysis confirmed quasi-planar structures for dimers **1–4** in the crystalline state. For example, the dihedral angles between the outer and inner phenyl rings in **1** (18.6°/23.0°; see Figure 2a) are in good agreement with the calculated optimized structure (22.8°). However, the dihedral angles between the inner phenyl rings obtained from the optimized structures of **1–4** (33.8°–35.1°) are not consistent with those observed in the crystal structures for **1** (0.0°) and **4** (49.7°). This discrepancy should probably be attributed to packing forces. The packing structures of dimers **1–4** in the crystals are all one-dimensional on-top  $\pi$ -stacks, with intermolecular distances of 3.72–3.79 Å (Figures 2b, 3c, S24 and S27), suggesting that compounds with this quasi-planar structural motif share a general tendency for

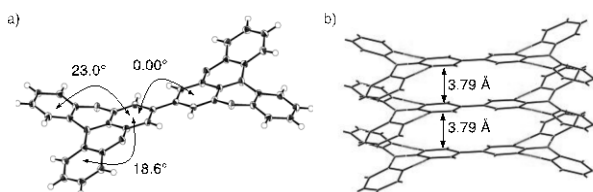


**Figure 2.** X-ray crystal structure of **1**: a) ORTEP drawing (50% probability for thermal ellipsoids) and b) packing structure.

the observed packing mode. DFT calculations at the B3LYP/6-31G(d) level suggested an inversion barrier for the flipping of the two phenyl rings in monomer **8a** of 9.1 kcal/mol (Figure S19), indicating that it should proceed easily in solution or under sublimation conditions. This flexibility should facilitate dense  $\pi$ -stacking in the on-top mode.

Interestingly, **2** exhibited crystalline polymorphism. Recrystallization from toluene (110–120 °C) resulted in the deposition of needle-like crystals (*P*-1), containing one-dimensional on-top  $\pi$ -stacks of **2** along the short *a*-axis (Figure 3a and 3c), similar to **1**, **3** and **4**. On the other hand, recrystallization from *o*-dichlorobenzene at higher temperature (140–160 °C) or sublimation (265 °C, 0.1 mmHg) provided plate-like crystals (*P*2<sub>1</sub>/a), in which two-dimensional  $\pi$ -stacks of **2** with a slipped arrangement were observed (Figures 3b and 3d). A determination of the face index confirmed that the longest axis in both types of crystals corresponds to the *a*-axis in  $\pi$ -stacking direction (Figure S29). Since neither a phase transition between the two crystals, nor a difference in melting point could be observed, we assume that the plate-like crystals form by entropy-driven processes at higher temperature.

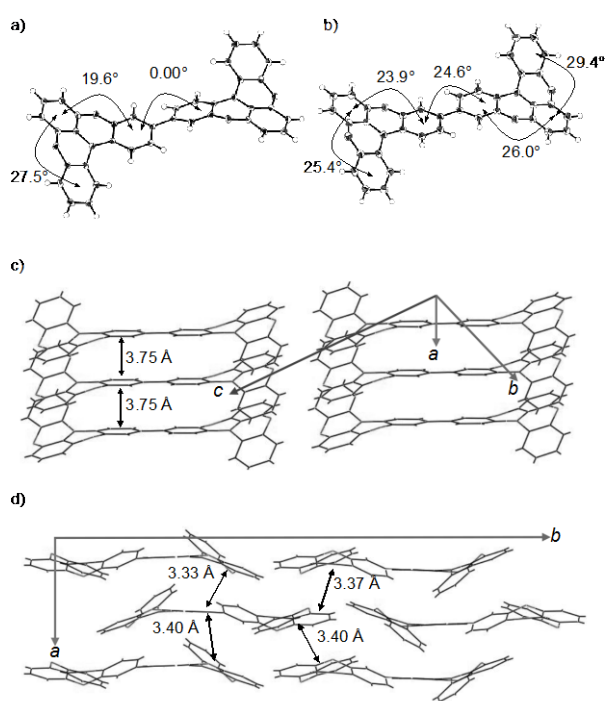


**Figure 3.** X-ray crystal structures of **2**: ORTEP drawings (50% probability for thermal ellipsoids) and packing structures for crystals obtained from toluene (a, c) or from *o*-dichlorobenzene (b, d).

To gain insight into the relationship between packing structures and carrier-transport properties, we conducted theoretical calculations at the PW91/DZP level and evaluated the charge transfer integrals (*J*) for crystals of **2** with different packing modes. For the one-dimensional  $\pi$ -stacking structure shown in Figure 3c, a large *J*-value (198 meV) was obtained for the hole-transfer integral in direction of the on-top  $\pi$ -stacking (*a*-axis), whereas small values were observed in the other directions (0.72–12.8 meV). For the two-dimensional  $\pi$ -stacking structure shown in Figure 3d, only moderate *J*-values (4.8–27.0 meV) were obtained, with less anisotropy in all possible directions (Tables S2 and S3).

In order to examine the relationship between packing structures and carrier-transport properties experimentally, time-resolved

microwave conductivity (TRMC) measurements<sup>[11]</sup> were carried out on several dozens of crystals, aligned on a quartz substrate (Figures 4a and 4b). TRMC measures the local mobility of charge carriers ( $\phi\Sigma\mu$ ) under an oscillating microwave electric field in the absence of contact between the semiconductors and the metal of electrodes, where  $\phi$  is defined as the charge carrier generation efficiency. It should be noted that the local mobility ( $\Sigma\mu$ ) obtained by TRMC is different from the bulk mobility in time-of-flight (TOF), space-charge-limited current (SCLC), and organic field-effect transistor (OFET) measurements, as the absence of the contact between the semiconductors and the electrode in TRMC allows the evaluation of the intrinsic charge carrier mobility and its anisotropy.<sup>[11]</sup> In the crystals with one-dimensional  $\pi$ -stacking, significant anisotropy of the intrinsic charge carrier mobility was observed. In direction of the on-top  $\pi$ -stacking ( $\phi\Sigma\mu = 6.1 \times 10^{-5} \text{ cm}^2/\text{Vs}$ ;  $\Sigma\mu = 0.34 \text{ cm}^2/\text{Vs}$ <sup>[12]</sup>), it was substantially higher compared to the other directions ( $\phi\Sigma\mu = 1.6\text{--}1.8 \times 10^{-5} \text{ cm}^2/\text{Vs}$ ;  $\Sigma\mu = 0.09\text{--}0.10 \text{ cm}^2/\text{Vs}$ <sup>[12]</sup>). No such anisotropy was observed in the crystals with two-dimensional  $\pi$ -stacks ( $\phi\Sigma\mu = 1.5\text{--}1.8 \times 10^{-5} \text{ cm}^2/\text{Vs}$ ;  $\Sigma\mu = 0.09\text{--}0.10 \text{ cm}^2/\text{Vs}$ <sup>[12]</sup>). These results are consistent with the results for the hole-transfer integrals.

In many of the organic electronic devices such as OLEDs and OPVs, the charge-transporting materials are used in form of films. Therefore, we also conducted TRMC measurements on vacuum deposited films (100 nm thickness) of **1** (Figure S31) and **2** on a quartz substrate (Figure 4c). Interestingly, we also observed a significant anisotropy of the carrier mobility. The mobility in perpendicular direction ( $\Sigma\mu_{\text{per}}$ ) to the quartz substrate (**1**: 0.98  $\text{cm}^2/\text{Vs}$ ; **2**: 0.57  $\text{cm}^2/\text{Vs}$ ) was approximately three times higher than that in parallel direction ( $\Sigma\mu_{\text{par}}$ ) to the substrate (**1**: 0.38  $\text{cm}^2/\text{Vs}$ ; **2**: 0.19  $\text{cm}^2/\text{Vs}$ ). In order to validate that the quasi-planar structure of **1** and **2** is responsible for this anisotropy, we conducted TRMC control measurements on vacuum deposited films of TPD, which has a corresponding non-planar structure (Figure S32). Albeit a minimal anisotropy of the carrier mobility was observed for this TPD film ( $\Sigma\mu_{\text{per}} = 0.53 \text{ cm}^2/\text{Vs}$ ;  $\Sigma\mu_{\text{par}} = 0.37 \text{ cm}^2/\text{Vs}$ ;  $\Sigma\mu_{\text{per}}/\Sigma\mu_{\text{par}} = 1.4$ ), it was significantly less prominent than those in films of **1** ( $\Sigma\mu_{\text{per}}/\Sigma\mu_{\text{par}} = 2.6$ ) and **2** ( $\Sigma\mu_{\text{per}}/\Sigma\mu_{\text{par}} = 3.0$ ).

To confirm this anisotropy, the ordering structure of **2** in thin film was investigated by X-ray diffraction studies. Vacuum deposited films of **2** did not exhibit any distinct diffraction peaks in measurements using a laboratory X-ray diffractometer with a sealed-tube X-ray generator (RIGAKU Ultima IV, Figure S33), suggesting that these films are essentially amorphous. However, in the two-dimensional grazing-incidence X-ray diffraction (2D-GIXD), using a synchrotron radiation source,<sup>[3e]</sup> we observed a diffraction halo corresponding to the  $\pi$ -stacking along the  $q_z$  axis (out-of-plane;  $q = 1.69\text{--}1.74 \text{ \AA}^{-1}$ , Figure 4d), whereas no distinct diffraction was observed in direction of the  $q_{xy}$  axis (in-plane). The determined  $\pi$ -stacking distance ( $d_\pi$ ) of 3.6–3.7 Å is in good agreement with the results obtained from the crystal structures. This suggests a horizontal molecular orientation (face-on), in which the  $\pi$ -stacking structure was retained to some extent, even in the amorphous state.<sup>[13]</sup> These results accordingly support the anisotropy of the carrier mobility observed by TRMC. In contrast, on the basis of variable angle spectroscopic ellipsometry measurements, non-planar TPD was reported to be randomly oriented in vacuum deposited films under similar conditions.<sup>[13b]</sup> It is therefore feasible to conclude that the anisotropy of the carrier mobility is most likely enhanced by the quasi-planar structural motif of oxygen-bridged triarylmines **1** and **2**.

In summary, we demonstrated that quasi-planar structures could be used as the key feature in the molecular design of triarylamines in order to obtain delocalized HOMOs and on-top  $\pi$ -stacks in the crystalline state, which leads to the observed high and anisotropic

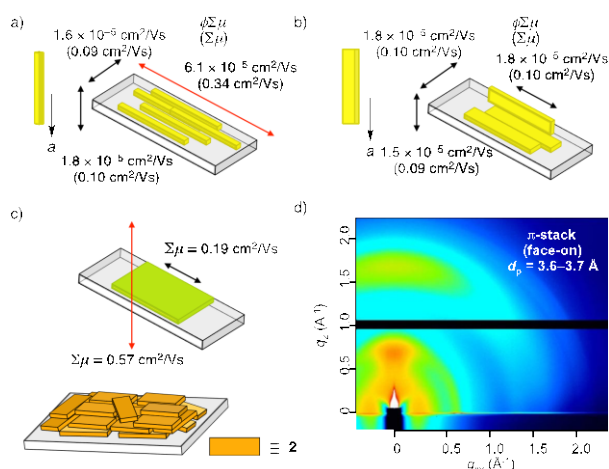


**Figure 4.** Anisotropy of the carrier mobility measured by TRMC for a) needle-like crystals, b) plate-like crystals and c) vacuum deposited films of **2** under excitation at 355 nm. d) 2D-GIXD image of a vacuum deposited film of **2**.

carrier mobilities in  $\pi$ -stacking direction. We also found that these compounds retain some extent of face-on  $\pi$ -stacking in amorphous films, thus facilitating out-of-plane charge transport. The properties exhibited by these quasi-planar triarylamine model compounds are expected to be extraordinarily beneficial for charge-transporting materials in OLEDs, OPVs, and perovskite-sensitized solar cells,<sup>[14]</sup> all of which require high levels of out-of-plane charge transport. Investigations concerning the applications of these types of charge-transporting materials are currently in progress in our laboratory and the results will be reported in due course.

Received: ((will be filled in by the editorial staff))

Published online on ((will be filled in by the editorial staff))

**Keywords:** Heterocycles · Semiconductors · Structure-function relationships · X-ray diffraction · Amorphous materials

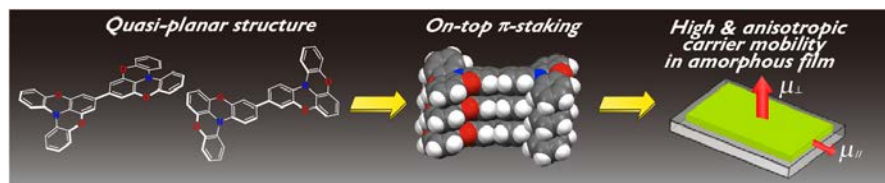
- [1] a) Y. Shirota, H. Kageyama, *Chem. Rev.* **2007**, *107*, 953–1010; b) L. Xiao, Z. Chen, B. Qu, J. Luo, S. Kong, Q. Gong, J. Kido, *Adv. Mater.* **2011**, *23*, 926–952.
- [2] a) J. E. Anthony, *Angew. Chem.* **2008**, *120*, 460–492; *Angew. Chem. Int. Ed.* **2008**, *47*, 452–483; b) H. Klauk, *Chem. Soc. Rev.* **2010**, *39*, 2643–2666; c) C. Wang, H. Dong, W. Hu, Y. Liu, D. Zhu, *Chem. Rev.* **2012**, *112*, 2208–2267.
- [3] a) B. Walker, C. Kim, T.-Q. Nguyen, *Chem. Mater.* **2011**, *23*, 470–482; b) A. Facchetti, *Chem. Mater.* **2011**, *23*, 733–758; c) A. Mishra, P. Bäuerle, *Angew. Chem.* **2012**, *124*, 2060–2109; *Angew. Chem. Int. Ed.* **2012**, *51*, 2020–2067; d) R. S. Kularatne, H. D. Magurudeniya, P. Sista, M. C. Biewer, M. C. Stefan, *J. Polym. Sci., Part A: Polym. Chem.* **2013**, *51*, 743–768; e) I. Osaka, T. Kakara, N. Takemura, T. Koganezawa, K. Takimiya, *J. Am. Chem. Soc.* **2013**, *135*, 8834–8837.
- [4] V. Coropceanu, J. Cornil, D. A. S. Filho, Y. Olivier, R. Silbey, J.-L. Brédas, *Chem. Rev.* **2007**, *107*, 926–952.
- [5] D. Holmes, S. Kumaraswamy, A. J. Matzger, K. P. C. Vollhardt, *Chem. –Eur. J.* **1999**, *5*, 3399–3412.
- [6] a) J. E. Anthony, J. S. Brooks, D. L. Eaton, S. R. Parkin, *J. Am. Chem. Soc.* **2001**, *123*, 9482–9483; b) X. Zhang, A. P. Coté, A. J. Matzger, *J. Am. Chem. Soc.* **2005**, *127*, 10502–10503; c) Q. Miao, X. Chi, S. Xiao, R. Zeis, M. Lefenfeld, T. Siegrist, M. L. Steigerwald, C. Nuckolls, *J. Am. Chem. Soc.* **2006**, *128*, 1340–1345.
- [7] a) *N,N'*-diphenyl-*N,N'*-di(*m*-tolyl)benzidine: Z. Zhang, Z. E. Burkholder, J. Zubieta, *J. Acta. Crystallogr., Sect. C: Cryst. Struct. Commun.* **2004**, *60*, o452–o454; b) 4,4-bis[*N*-(1-naphthyl)-*N*-phenylamino]-biphenyl: L.-Q. Huang, Q.-Y. Cao, C. Yi, C.-J. Yang, X.-C. Gao, *Acta. Crystallogr., Sect. E: Struct. Rep. Online* **2006**, *62*, o2075–o2076.
- [8] T. Yamada, T. Sato, K. Tanaka, H. Kaji, *Org. Electron.* **2010**, *11*, 255–265.
- [9] M. Kuratsu, M. Kozaki, K. Okada, *Chem. Lett.* **2004**, *33*, 1174–1175.
- [10] J. Pommerehne, H. Vestweber, W. Guss, R. F. Mahrt, H. Bässler, M. Porsch, J. Daub, *Adv. Mater.* **1995**, *7*, 551–554.
- [11] a) A. Saeki, Y. Koizumi, T. Aida, S. Seki, *Acc. Chem. Res.* **2012**, *45*, 1193–1202 and references cited therein; b) A. Saeki, S. Seki, T. Takenobu, Y. Iwasa, S. Tagawa, *Adv. Mater.* **2008**, *20*, 920–923; c) Y. Yasutani, A. Saeki, T. Fukumatsu, Y. Koizumi, S. Seki, *Chem. Lett.* **2013**, *42*, 19–21.
- [12] The charge carrier generation efficiency ( $\phi = 1.76 \times 10^{-4}$  for **2**) was measured for the vacuum deposited film and was subsequently used to estimate the local mobility  $\Sigma\mu$  in the crystals.
- [13] a) D. Yokoyama, *J. Mater. Chem.* **2011**, *21*, 19187–19202 and references cited therein; b) D. Yokoyama, A. Sakaguchi, M. Suzuki, C. Adachi, *Appl. Phys. Lett.* **2008**, *93*, 173302.
- [14] a) A. Kojima, K. Teshima, Y. Shirai, T. Miyasaka, *J. Am. Chem. Soc.* **2009**, *131*, 6050–6051; b) M. M. Lee, J. Teuscher, T. Miyasaka, T. N. Murakami, H. J. Snaith, *Science* **2012**, *338*, 643–647; c) J. H. Heo, S. H. Im, J. H. Noh, T. N. Mandal, C.-S. Lim, J. A. Chang, Y. H. Lee, H. Kim, A. Sarkar, M. K. Nazeeruddin, M. Grätzel, S. I. Seok, *Nat. Photonics* **2013**, *7*, 486–491.

## Heterocycles

Prof. Dr. Atsushi Wakamiya,\* Hidetaka Nishimura, Dr. Tatsuya Fukushima, Furitsu Suzuki, Dr. Akinori Saeki, Prof. Dr. Shu Seki, Dr. Itaru Osaka, Prof. Dr. Takahiro Sasamori, Dr. Michihisa Murata, Prof. Dr. Yasujiro Murata,\* and Prof. Dr. Hironori Kaji\*\_\_\_\_\_

**Page – Page**

On-Top  $\pi$ -Stacking of Quasi-Planar Molecules in Hole-Transporting Materials: Inducing Anisotropic Carrier Mobility in Amorphous Films



Dimers of partially oxygen-bridged triarylamines were designed and synthesized as hole-transporting materials. X-ray structural analyses revealed that these compounds form on-top  $\pi$ -stacking aggregates in the crystalline state. TRMC measurements exhibited that high levels of anisotropic charge-transport were induced in direction of the  $\pi$ -stacking. Surprisingly, even in vacuum deposited amorphous films, these compounds retained some of the face-on  $\pi$ -stacking, thus facilitating an out-of-plane carrier mobility.